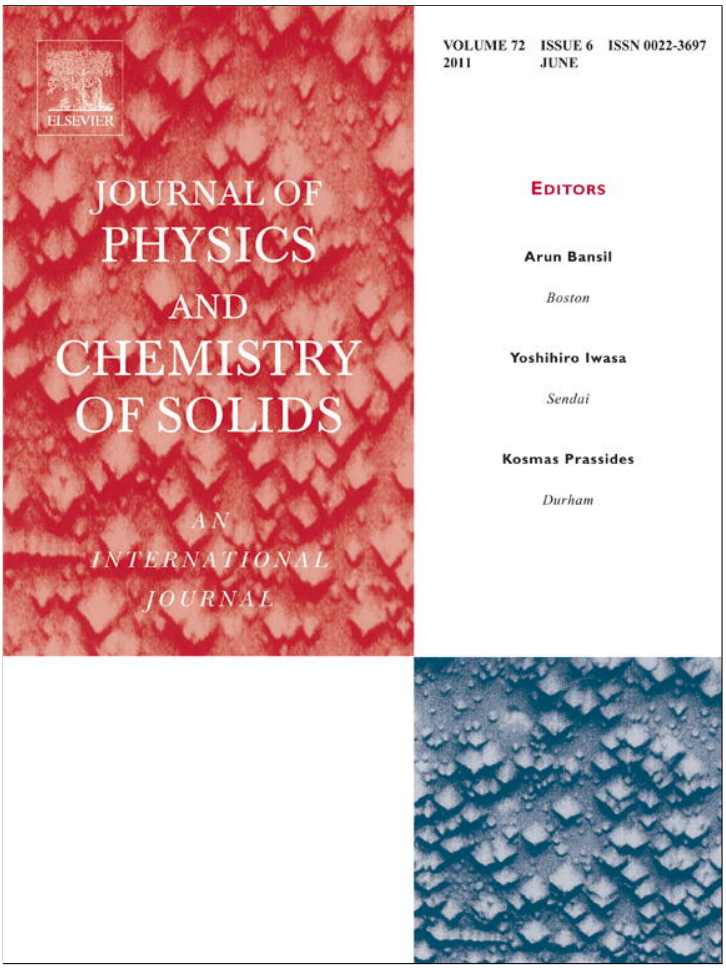

Journal of Physics and Chemistry of Solids 72 (2011) 736–739

Contents lists available at ScienceDirect

Journal of Physics and Chemistry of Solids

journal homepage: www.elsevier.com/locate/jpcs

High pressure X-ray diffraction study of potassium azide

Cheng Ji [a], Fuxiang Zhang [b], Dongbin Hou [a], Hongyang Zhu [a], Jianzhe Wu [a], Ming-Chien Chyu [a], Valery I. Levitas [c], Yanzhang Ma [a,*]

[a] Department of Mechanical Engineering, Texas Tech University, Lubbock, TX 79409-1021, USA
[b] Department of Geological Sciences, University of Michigan, Ann Arbor, MI 48109-1005, USA
[c] Department of Mechanical Engineering, Aerospace Engineering, and Material Science and Engineering, Iowa State University, Ames, Iowa 50011, USA

ARTICLE INFO

Article history:
Received 21 November 2010
Received in revised form
29 January 2011
Accepted 10 March 2011
Available online 21 March 2011

Keywords:
A. Diamond anvil cell
B. Synchrotron X-ray diffraction
C. Anisotropic compressibility
D. Phase transition

ABSTRACT

Crystal structure and compressibility of potassium azide was investigated by *in-situ* synchrotron powder X-ray diffraction in a diamond anvil cell at room temperature up to 37.7 GPa. In the body-centered tetragonal (bct) phase, an anisotropic compressibility was observed with greater compressibility in the direction perpendicular to the plane containing N_3^- ions than directions within that plane. The bulk modulus of the bct phase was determined to be 18.6(7) GPa. A pressure-induced phase transition may occur at 15.5 GPa.

1. Introduction

Metal azides, which exhibit a comparatively rare set of physical and chemical properties have drawn considerable attention [1]. As their principle characteristic, the decomposition upon external stimulations (impact, heat, irradiation, etc.) has been studied extensively [2]. Their practical applications include explosives and pure nitrogen sources. Scientifically, metal azides are model systems to study the complex nature of chemical bonding as their spatial symmetry and internal molecular structure make them logical candidates for such studies following alkali halides and cyanides. Both experimental and theoretical studies have been undertaken on the structural, electronic, and optical properties of metal azides [3–7].

Alkali azides, a relatively stable species among metal azides undergo a variety of phase transitions stimulated by either temperature or pressure change, a phenomenon that has been intensively studied [8–11]. A topic of recent interest of alkali azide is the polymerization of N_3^- ions to form a highly energetic density material (HEDM) through high pressure treatment. This is pioneered by studies of nitrogen, of which, a polymeric phase under high pressure was first predicted [12] and later synthesized [13]. The N_3^- ions in sodium azide were found to transform into larger nitrogen clusters and then polymeric nitrogen nets [10]. A high pressure study on lithium azide (LiN_3) also predicted the formation of a polymeric nitrogen network with further compression beyond its pressure range studied [14]. Thus, a high pressure study of potassium azide (KN_3) would help in further understanding of the pressure effect on possible formation of polymeric nitrogen.

At ambient condition, KN_3 has a body-centered tetragonal (bct) lattice of space group I4/mcm-D_{4h} with potassium (K), nitrogen 1 (N1), and nitrogen 2 (N2) atoms located on the 4c, 4a, and 8h wyckoff positions, respectively [7] (Fig. 1). The N_3^- ions, linear and symmetric, occupy alternate [1 1 0] and [1 $\bar{1}$ 0] directed position in the crystal to form N_3^- ion planes ((0 0 1) and (0 0 2) planes) separated by layers of K ions. The previous high pressure studies of KN_3 have been done using IR spectroscopy up to 2.5 GPa [15], Raman scattering up to 2.0 [16] and 4.0 GPa [17], and single crystal X-ray diffraction up to 2.2 GPa at room temperature and 7 GPa at 373 K [18]. No phase transition at these P–T conditions was reported. To investigate the structure and compressibility of KN_3 at higher pressures, powdered KN_3 was studied using synchrotron angle-dispersive X-ray diffraction (SADXRD) at room temperature up to 37.7 GPa in the present work.

2. Experimental methods

Powdered KN_3 was synthesized on a small scale by a replacement reaction [1]. Two runs of high pressure experiments were performed in a symmetric diamond anvil cell with flat diamond culets of 400 μm diameter. In the first run, a sheet of rhenium

* Corresponding author. Tel.: +806 742 3563x243; fax: +806 742 3540.
E-mail address: y.ma@ttu.edu (Y. Ma).

0022-3697/$ - see front matter © 2011 Elsevier Ltd. All rights reserved.
doi:10.1016/j.jpcs.2011.03.005

metal was pre-indented to a thickness of about 40 μm, and a hole with a diameter of 120 μm drilled at the center of the dent by an electrical discharge machine served as the sample chamber. The mortar-ground sample was hand-compacted into a flake and loaded into the sample chamber. A ruby chip was then loaded between the sample flake and the edge of the gasket hole for pressure calibration by observing the spectral shift of the sharp fluorescent R1 ruby line [19]. The sample chamber was filled with a mixture of methanol and ethanol at a ratio of 4:1 as the pressure-transmitting medium. In the second run, all the sample loading setups are the same except that the selections of gasket and pressure media were stainless steel (pre-indented to about 90 μm) and mineral oil, respectively. The first run of high pressure *in-situ* SADXRD measurements was carried out at the B2 station of Cornell High Energy Synchrotron Source (CHESS) by means of a monochromatic X-ray beam with a wavelength of 0.4860 Å and a 40×40 μm^2 spot size. The Debye rings were recorded using a Mar3450 image plate. The second run of SADXRD experiments was carried out at X17C station of National Synchrotron Light Source (NSLS), Brookhaven National Laboratory, using a monochromatic beam with a wavelength of 0.4066 Å and a spot size of 20×25 μm^2. The diffraction pattern was recorded using a Mar charge-coupled device detector with a smaller sample to detector distance compared with the first run to increase the collected diffraction intensity. Using the software FIT 2D [20], these diffraction images were integrated to two-dimensional diffraction patterns. Cell parameters were calculated from the first run of data by software Refine [21] using peak positions identified by PEAKFIT v4.11 (Systat, Richmond, CA). Since the relative intensity information was distorted by weak diffraction in the data of first run, the data of second run with much stronger intensity were analyzed using the Rietveld refinement technique [22] with Fullprof software [23].

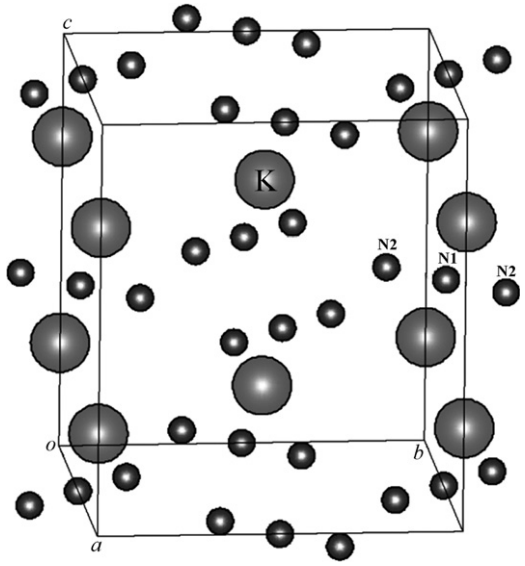

Fig. 1. Crystal structure of KN_3 at ambient condition. Big spheres and small spheres represent K and N atoms, respectively.

3. Results and discussion

The lattice constants obtained at ambient condition, $a=6.1109(4)$ Å and $c=7.0975(5)$ Å, are in agreement with the results in literature ($a=6.1129$ Å and $c=7.0943$ Å) [7]. The representative XRD patterns obtained at various pressures are shown in Fig. 2. Peaks are indexed as (1 1 0), (2 0 0), (1 1 2), (2 1 1), (2 0 2), (2 2 0), (3 1 0), (2 2 2), (2 1 3), (0 0 4), (3 1 2), (3 2 1), and (1 1 4) of the bct phase at ambient pressure. Fig. 3 shows the

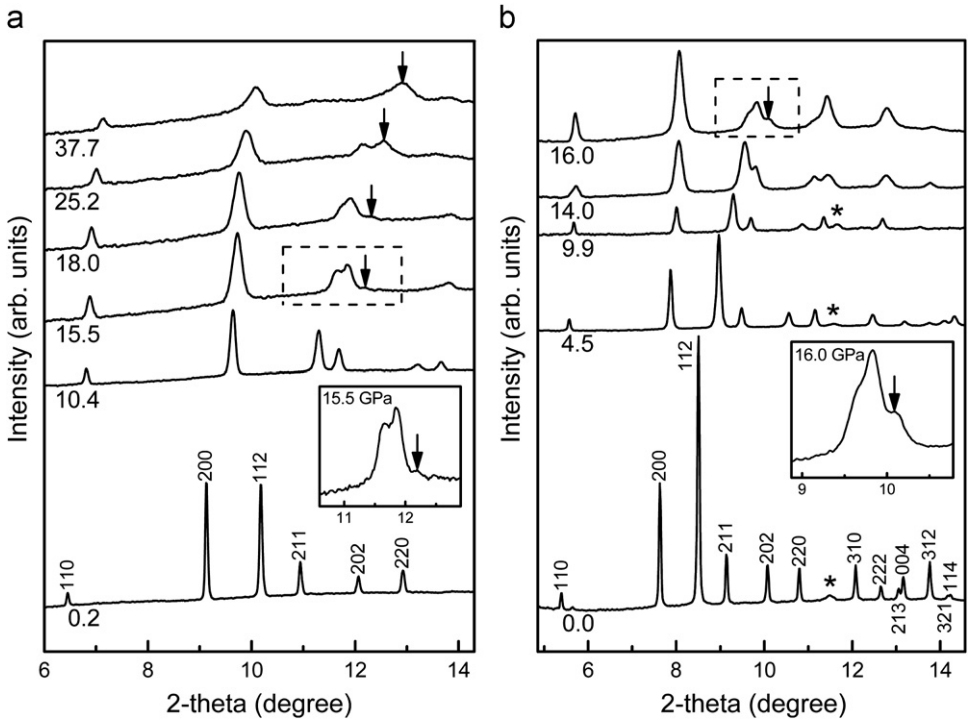

Fig. 2. Selected diffraction patterns under pressures. Numbers under diffraction patterns on the left are pressures in GPa. New peak is indicated by arrows. (a) Patterns obtained from the first run. A magnified view of the 15.5 GPa pattern in the dashed frame is shown in the inset. Intensity of patterns from 15.5 GPa to 37.7 GPa are doubled artificially for the purpose of illustration. (b) Patterns obtained from the second run. Inset is a magnified view of the 16.0 GPa pattern in the dashed frame. Asterisk (*) marked peak is the (1 1 0) peak of α-Fe gasket.

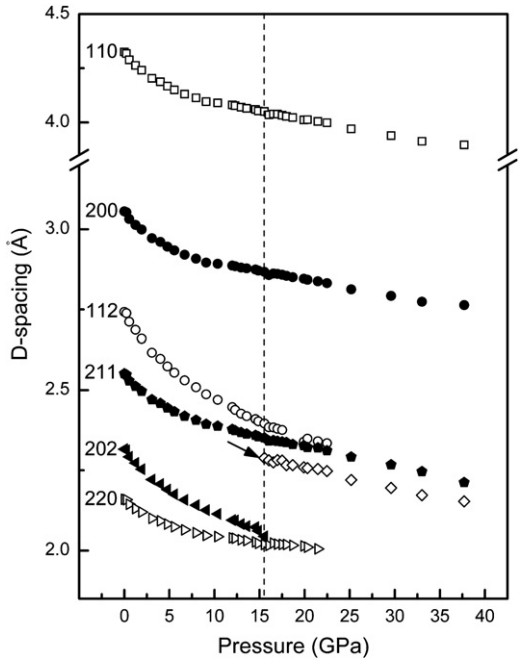

Fig. 3. D-spacing variation with pressure. New peak is indicated by an arrow and dashed line serves as a possible phase boundary.

Table 1
Variation of cell parameters and unit cell volume of KN_3 under pressures. Numbers in parentheses are the calculated standard deviations.

GPa	a (Å)	c (Å)	V (Å^3)
0.0	6.1109(4)	7.0975(5)	265.04(3)
0.2	6.1056(2)	7.0832(6)	264.05(2)
0.6	6.0645(2)	7.0008(7)	257.47(2)
1.2	6.0264(4)	6.923(1)	251.42(4)
1.9	5.9965(5)	6.831(2)	245.64(5)
3.1	5.9419(7)	6.688(2)	236.14(7)
4.0	5.9188(8)	6.627(2)	232.14(7)
4.8	5.8903(6)	6.549(2)	227.21(6)
5.6	5.8673(6)	6.484(2)	223.21(5)
6.7	5.8400(6)	6.404(2)	218.42(5)
8.0	5.8147(9)	6.333(2)	214.13(8)
9.1	5.7904(8)	6.262(2)	209.96(6)
10.4	5.782(1)	6.199(3)	207.2(1)
12.0	5.769(3)	6.106(7)	203.2(2)
12.3	5.766(1)	6.087(2)	202.35(8)
13.0	5.753(2)	6.042(5)	199.2(2)
13.6	5.746(3)	6.014(6)	198.6(2)
14.6	5.740(2)	5.989(4)	197.4(1)
14.9	5.736(2)	5.968(4)	196.3(1)

pressure dependence of d-spacing, peaks consistently shift to lower d-spacing values with (1 1 2) and (2 1 1) peaks moving closer, and (2 0 2) and (2 2 0) peaks showing the same due to the different compression ratio between a-axis and c-axis. In both the runs below 15.5 GPa, all existing peaks can be well indexed into the ambient bct phase; the observed weakening and broadening of peaks are attributed to the thinning of sample and the deviatoric stress, respectively. Additionally, it can be noticed in Fig. 2(b) that the relative intensity between (2 0 0) and (1 1 2) keeps changing with pressure and gets reversed around 14.0 GPa. Since no significant preferred orientation was observed in diffraction images, the contradiction between the reversal of relative intensities and calculation of Fullprof with the bct model [the intensity of (1 1 2) should be much larger than that of (2 0 0)] cannot be solely attributed to an preferred orientation effect and

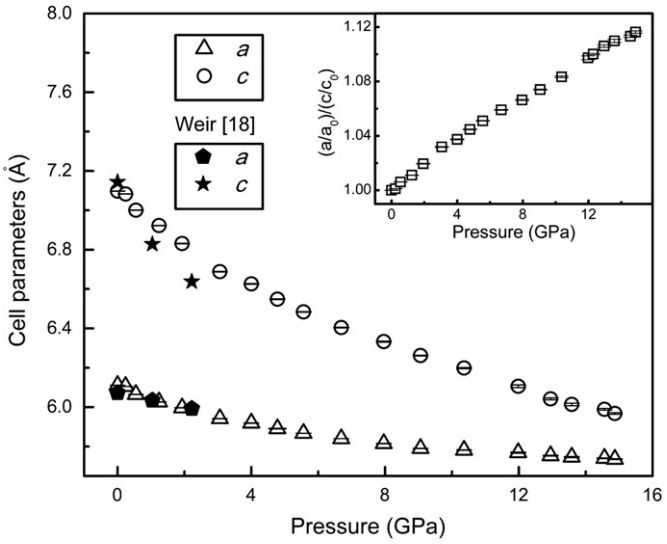

Fig. 4. Cell parameter dependence on pressure. Inset shows the ratio between normalized cell parameters at pressures and error bars show the standard deviations resulted from the calculation.

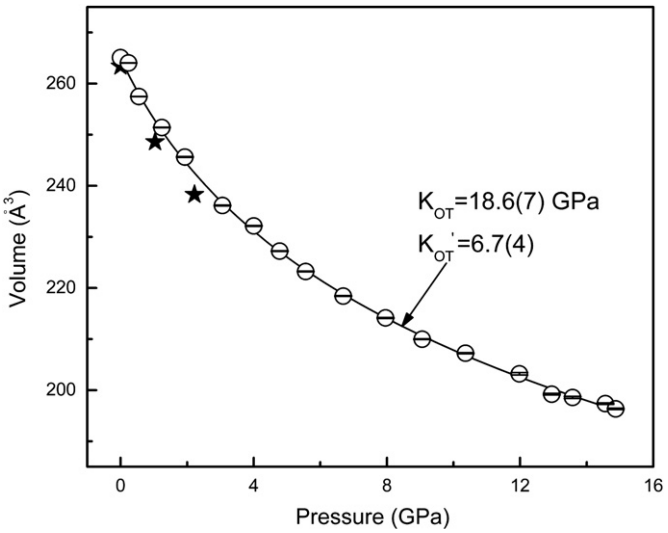

Fig. 5. Unit cell volume dependence on pressure. Error bars show the standard deviations resulted from the calculation and star represents results from Weir et al. [18].

can possibly be explained by splitting of the K atomic position from 4a to 8f site together with slight release of N according to the refinement results. With further compression, a new peak that cannot be indexed in the ambient bct phase emerged in both runs at 15.5 GPa [Fig. 2(a)] and 16.0 GPa [Fig. 2(b)]. From 15.5 to 37.7 GPa, the new peak intensifies [Fig. 2(a)] while the first two high d-spacing peaks continue to shift consistently to lower d-spacing values (Fig. 3). There are two possible explanations for this phenomenon. The first one is a phase transition starting at 15.5 GPa with subtle and sluggish structural change in the subsequent pressurization process. But we are unable to identify a structure model for patterns at these pressures. The second explanation is a decomposition induced by both pressurization and X-ray illumination. The defects generated by N release may be unstable under pressure and induce decomposition upon further compression, which might explain the emerging of the new peak.

The cell parameters at different levels of pressure up to 14.9 GPa are listed in Table 1 and plotted in Fig. 4. Compared with the previous study by Weir et al. [18], the current *a* result is in good agreement, while discrepancies exist in *c* result. Since there was insufficient data to do a meaningful least-squares refinement to calculate the cell parameters in the study of Weir et al. [18], the discrepancies may be attributed to their big calculation errors. According to the inset in Fig. 4, the $(a/a_0)/(c/c_0)$ ratio keeps increasing with pressure, reaching a maximum value of 1.12 at 14.9 GPa. It shows that the *c*-axis along the inter-plane direction of the N_3^- ion planes is more compressible than the *a*-axis along the intra-plane direction. In addition, K–K distance along the [0 0 1] direction ($d_{(001)}/2$) is shorter than that along the [1 1 0] (or [1 $\bar{1}$ 0]) direction ($\sqrt{2}d_{(100)}/2$) at a given pressure. By considering this fact and the observation that the *c*-axis is actually more compressible than the *a*-axis, it can be implied that the repulsions between N_3^- ions dominate the compressibility of the KN_3 crystal. Similar anisotropic compressibilities were also observed in thallium azide (TlN_3) at ambient pressure [18] and potassium hydrogen fluoride (KHF_2) at high pressures [24], of which both are isostructural with KN_3. LiN_3, monoclinic with N_3^- ions lying in the *ac* plane was found to have its deformation concentrated within the basal *ab* plane upon compression [14]. These published data and our data suggest that the compression within the plane containing anion groups is more difficult for these univalent linear anion compounds.

Variation in the KN_3 unit cell volume with pressure is shown in Fig. 5. The volume is found to reduce by 28.6% at 14.9 GPa compared with the ambient value. Fitting the data to the third-order isothermal Birch–Murnaghan equation of state [25] yields a bulk modulus (K_{OT}) of 18.6(7) GPa with the pressure derivative ($K_{OT'}$) of 6.7(4) for the bct phase of KN_3. These values are close to those of LiN_3, reported as $K_{OT}=19.1$ GPa with $K'_{OT}=7.3$ [14].

4. Conclusion

KN_3 was compressed to 37.7 GPa with *in-situ* synchrotron powder X-ray diffraction measurements. In the bct phase, compression of KN_3 is anisotropic with the N_3^- ions plane more difficult to compress in the intra-plane direction than the inter-plane direction. A third-order Birch–Murnaghan equation of state fitting resolves a bulk modulus of 18.6(7) GPa with the pressure derivative of 6.7(4). KN_3 may undergo a phase transition at 15.5 GPa.

Acknowledgments

The authors thank Dr. Zhongwu Wang at CHESS and Dr. Zhiqiang Chen at NSLS for their technical helps. This work is supported by the Defense Threat Reduction Agency (HDTRA1–09–0034), the Army Research Office (W911NF-09–1–0001), and the National Science Foundation (DMR-0619215).

References

[1] H.D. Fair, R.F. Walker, (Eds.), Energetic materials, in: Physics and Chemistry of the Inorganic Azides, vol. 1, 1977.
[2] B.L. Evans, A.D. Yoffe, P. Gray, Physics and chemistry of the inorganic azides, Chem. Rev. 59 (1959) 515–568.
[3] W. Zhu, J. Xiao, H. Xiao, Comparative first-principles study of structural and optical properties of alkali metal azides, J. Phys. Chem. B 110 (2006) 9856–9862.
[4] A.B. Gordienko, Y.N. Zhuravlev, A.S. Poplavnoi, Electronic structure of metal azides, Phys. Status Solidi B 198 (1996) 707–719.
[5] R.J. Colton, J.W. Rabalais, Electronic structure of some inorganic azides from X-ray electron spectroscopy, J. Chem. Phys. 64 (1976) 3481–3486.
[6] A. Danemar, B.S.H. Royce, D.O. Welch, Born model calculations of the properties of the alkali azides I. Cohesive energies, lattice parameters, and specific volumes, Phys. Status Solidi B 70 (1975) 663–671.
[7] U. Mueller, Crystal structure refinements of potassium, rubidium, cesium, and thallium azides, Z. Anorg. Allg. Chem. 392 (1972) 159–166.
[8] H.J. Mueller, J.A. Joebstl, High-temperature modifications of alkali azides, Z. Kristallogr. Kristallgeom. Kristallphys. Kristallchem. 121 (1965) 385–391.
[9] G.E. Pringle, D.E. Noakes, Crystal structures of lithium, sodium, and strontium azides, Acta Crystallogr. Sect. B 24 (1968) 262–269.
[10] M.I. Eremets, M.Y. Popov, I.A. Trojan, V.N. Denisov, R. Boehler, R.J. Hemley, Polymerization of nitrogen in sodium azide, J. Chem. Phys. 120 (2004) 10618–10623.
[11] C.W.F.T. Pistorius, Phase diagrams to high pressures of the univalent azides belonging to the space group D4h18-I4/mcm, J. Chem. Phys. 51 (1969) 2604–2609.
[12] A.K. McMahan, R. LeSar, Pressure dissociation of solid nitrogen under 1 Mbar, Phys. Rev. Lett. 54 (1985) 1929–1932.
[13] M.I. Eremets, A.G. Gavriliuk, I.A. Trojan, Single-crystalline polymeric nitrogen, Appl. Phys. Lett. 90 (2007) 171904/171901–171904/171903171904/171901–171904/171903.
[14] S.A. Medvedev, I.A. Trojan, M.I. Eremets, T. Palasyuk, T.M. Klapoetke, J. Evers, Phase stability of lithium azide at pressures up to 60 GPa, J. Phys. Condens. Matter 21 (2009) 195404/195401–195404/195405195404/195401–195404/195405.
[15] A. Klopsch, E. Hellner, K. Dehnicke, Infrared spectra of transition metal complexes and azides under high pressure, Ber. Bunsenges. Phys. Chem. 80 (1976) 500–503.
[16] M.Y. Khilji, W.F. Sherman, G.R. Wilkinson, Variable temperature and pressure Raman spectra of potassium azide KN3, J. Raman Spectrosc. 12 (1982) 300–303.
[17] C.W. Christoe, Z. Iqbal, Raman scattering in alkali azides at high pressures, Chem. Phys. Lett. 39 (1976) 511–514.
[18] C.E. Weir, S. Block, G.J. Piermarini, Compressibility of inorganic azides, J. Chem. Phys. 53 (1970) 4265–4269.
[19] H.K. Mao, J. Xu, P.M. Bell, Calibration of the ruby pressure gage to 800 kbar under quasi-hydrostatic conditions, J. Geophys. Res. B 91 (1986) 4673–4676.
[20] A.P. Hammersley, ESRF Internal Report, ESRF98HA01T, Fit2D9.129 Reference Manual V3.1, 1998.
[21] T. Laetsch, R. Downs, Abstracts from the 19th General Meeting of the International Mineralogical Association, Kobe, Japan, 2006.
[22] H.M. Rietveld, Profile refinement method for nuclear and magnetic structures, J. Appl. Crystallogr. 2 (1969) 65–71.
[23] J. Rodriguez-Carvajal, FULLPROF2K, France, 2001.
[24] A.G. Christy, S.M. Clark, Equation of state of potassium hydrogen fluoride to 12.0.3 GPa and stability of I4/mcm structure to 50 GPa: an energy-dispersive x-ray diffraction study, J. Solid State Chem. 125 (1996) 171–177.
[25] F. Birch, Finite elastic strain of cubic crystals, Phys. Rev. 71 (1947) 809–824.